

- (16) Harkema, S.; Gaymans, R. J.; van Hummel, G. J.; Zylberlicht, D. *Acta Crystallogr., Sect. B* 1979, 35, 506. Hummel, J. P.; Flory, P. J. *Macromolecules* 1980, 13, 479.
- (17) Krigbaum, W. R.; Chatani, Y.; Barber, P. G. *Acta Crystallogr., Sect. B* 1970, 26, 97.
- (18) Martins, A. F.; Ferreira, J. B.; Volino, F.; Blumstein, A.; Blumstein, R. B. *Macromolecules* 1983, 16, 279.
- (19) Abe, A. *J. Am. Chem. Soc.* 1984, 106, 14.
- (20) Flory, P. J. "Statistical Mechanics of Chain Molecules"; Interscience: New York, 1969; p 173.
- (21) This value is determined from both  $^1\text{H}$  NMR and  $^2\text{H}$  NMR measurements of the polymer with  $(\text{CD}_2)_{10}$  spacer of a relatively low molecular weight.<sup>22</sup> It is somewhat larger than  $s \sim 0.6$  obtained in ref 11 from the measurement of diamagnetic anisotropy of a high molecular weight polymer. This difference is most likely due to the difficulty in achieving complete alignment of the high molecular weight polymer under the applied magnetic field in the latter experiment.
- (22) Bruckner, S.; Scott, J. C.; Yoon, D. Y.; Griffin, A. C., in preparation.

## Theory of Micelle Formation in Block Copolymer-Homopolymer Blends

Mark Douglas Whitmore<sup>†</sup> and Jaan Noolandi\*

Xerox Research Centre of Canada, 2660 Speakman Drive,  
Mississauga, Ontario, Canada L5K 2L1. Received April 23, 1984

**ABSTRACT:** The structural parameters of monodisperse AB diblock copolymer micelles in homopolymer of type A are derived by minimizing a simple free energy expression. The core is found to consist almost entirely of B blocks of the copolymer molecules, with radius  $l_B$  depending primarily on the degree of polymerization of that block,  $Z_{CB}$ .  $l_B$  scales as  $l_B \propto Z_{CA}^\omega Z_{CB}^\nu$ , where  $Z_{CA}$  is the dp of the copolymer A block,  $0.67 \lesssim \nu \lesssim 0.76$ , and  $\mu$  is small and negative,  $-0.1 \lesssim \mu \lesssim 0$ . Similarly the corona thickness  $l_A$  is found to depend primarily on the copolymer A block, varying as  $Z_{CA}^\omega$ , with  $0.5 \lesssim \omega \lesssim 0.86$ . The physical origin of these exponents is discussed, and the stretching parameters of the polymer chains are obtained. The swelling of the corona by homopolymer of low molecular weight ( $Z_{HA} \ll Z_{CA}$ ) is also described. The theory is applied to an analysis of recent small-angle neutron scattering data for the polystyrene/polybutadiene system, and excellent agreement with experiment is demonstrated. The critical micelle concentration is calculated and shown to be dominated by an exponential dependence on  $\chi_{AB} Z_{CB}$ , where  $\chi_{AB}$  is the Flory-Huggins interaction parameter. As a general result, the importance of the copolymer composition is emphasized; every property of the system depends on either  $Z_{CA}$  or  $Z_{CB}$  or both, but never on just the total molecular weight.

### 1. Introduction

Recent experimental work<sup>1</sup> on the structure of block copolymer-homopolymer blends using small-angle neutron scattering (SANS) affords a unique opportunity to test modern theories of micelle formation in these systems. Previously we have developed a simple model of AB diblock copolymer micelles in selective small-molecule solvents.<sup>2</sup> In this paper our earlier work is generalized to include "dilute solid solutions" of diblock copolymers of arbitrary composition in a homopolymer matrix. Remarkably good agreement with the SANS measurements of Selb et al.<sup>1</sup> is obtained. There are no fitted parameters in our model.

Our model assumes that both the corona and core of the micelle are homogeneous, as shown in Figure 1, allowing us to write down the free energy density of the system quite simply without any integrals over density profiles. Minimization of the free energy with respect to the structural and compositional parameters of the micelle gives the optimum values of the core and corona radii, as well as the aggregation number of copolymer molecules per micelle. These quantities are shown to depend not only on the total molecular weight of the copolymer, but, more significantly, on the individual blocks CA and CB.

As an added result, we find that allowing for copolymer in solution between micelles has very little effect on the calculated size parameters, but it is important in determining the critical micelle concentration.<sup>3</sup>

In section 2 we begin with a detailed description of the model. The general trends with the molecular weights of

each block of the copolymer and of the homopolymer are explored in section 3a. We find that the homopolymer is almost completely excluded from the core of the micelle for a wide range of molecular weights. The core radius and corona thickness are found to scale primarily with the molecular weights of the CB and CA blocks of the copolymer, respectively. The values of the important exponents are derived from the analytical expressions given in section 2. In particular the penetration and stretching of the A blocks of the corona by homopolymer of small molecular weight is discussed quantitatively. Section 3b and Tables I-V compare the results of our calculations for the system of polystyrene/polybutadiene copolymers in polybutadiene homopolymers with the SANS measurements of Selb et al.<sup>1</sup> The critical micelle concentration is discussed in section 4, and section 5 contains the conclusions.

### 2. Description of Model

Each micelle is modeled by a spherical core of radius  $l_B$  surrounded by a corona of thickness  $l_A$ , as indicated in Figure 1. The unit cell is a sphere of radius  $R$  and is defined as the volume which on average contains one micelle. Each of the three regions is assumed uniform throughout. The number fraction of copolymers which remain in solution in region 3 between the micelles is denoted by  $F_3^C$ , while  $F_M^C = 1 - F_3^C$  is the fraction in the micelles. The copolymers which are in micelles are assumed to have their joints localized at the interface, with the polystyrene block, labeled CB, stretched in toward the center, and the polybutadiene, or CA block, in the corona. The core radius  $l_B$  and the corona thickness  $l_A$  are proportional to the average end-to-end distances of the CB and CA blocks, respectively. Polybutadiene homo-

<sup>†</sup> Permanent address: Department of Physics, Memorial University of Newfoundland, St. John's, Newfoundland, Canada A1B 3X7.

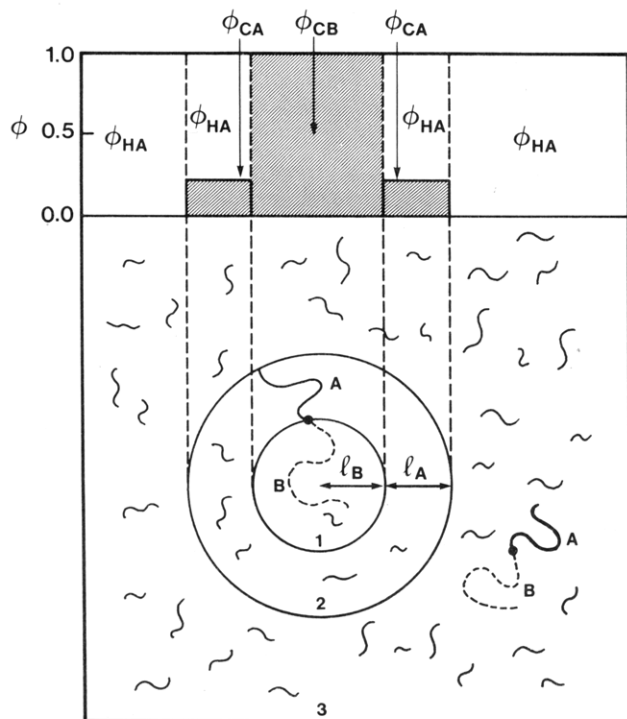


**Figure 1.** Cross section of a spherical micelle consisting of AB diblock copolymers in a matrix of A homopolymer. Except for very low molecular weight homopolymers, the core (region 1) was found to consist almost entirely of B blocks, so that  $\varphi_{CB}^{(1)} \approx 1$ ,  $\varphi_{HA}^{(1)} \approx 0$ . Furthermore, very little copolymer was found to remain in solution (region 3), so that  $\varphi_C^{(3)} \approx 0$ ,  $\varphi_{HA}^{(3)} \approx 1$ . In the corona (region 2), the stretching of the A block was in the range  $1 \leq \alpha_A \leq 2$ , with volume fractions generally falling in the range  $0.05 \leq \varphi_{CA}^{(2)} \leq 0.25$ ,  $\varphi_{HA}^{(2)} = 1 - \varphi_{CA}^{(2)}$ . All calculations were done for polystyrene/polybutadiene copolymers and polybutadiene homopolymers, with the identification A  $\equiv$  butadiene, B  $\equiv$  styrene.

polymers, labeled HA, can be in any of the three regions; the fraction of homopolymer in each is denoted  $F_i^{HA}$ .

For a given overall volume fraction of copolymer, the free energy of the micelles relative to a random uniform distribution of copolymers is calculated. This theoretical expression is then minimized with respect to the independent parameters which determine the micelle dimensions, as well as the amount of homopolymer and copolymer in each of the three regions. If the free energy is positive, the micelles are unstable or metastable; if it is negative, then they are stable. The critical concentration  $\varphi_c^{crit}$  is essentially the overall volume fraction of copolymer  $\varphi_c^0$  for which this free energy difference vanishes. Thus, our model is a generalization of the earlier work of Noolandi and Hong,<sup>2</sup> the major differences being that homopolymer rather than solvent is used, some copolymer can remain in solution between the micelles, i.e., in region 3, and in particular we treat arbitrary copolymer composition; i.e., we do not restrict ourselves to the case  $Z_{CA} = Z_{CB}$ .

The model also extends the work of Leibler, Orland, and Wheeler,<sup>3</sup> who allowed for some copolymer to remain in solution, but neglected localization of the copolymer joints to the interfacial region of the micelle, assumed no homopolymer penetrated into the core, and kept  $Z_{CA} = Z_{CB}$ .

The polymers are assumed to be incompressible, so that in each region the volume fractions sum to unity:

$$\begin{aligned}\varphi_{CB}^{(1)} + \varphi_{HA}^{(1)} &= 1 \\ \varphi_{CA}^{(2)} + \varphi_{HA}^{(2)} &= 1 \\ \varphi_C^{(3)} + \varphi_{HA}^{(3)} &= 1\end{aligned}\quad (2-1)$$

In these equations the superscript specifies the region and for each copolymer block  $\varphi_{C\kappa}^{(i)} = \rho_{C\kappa}^{(i)} / \rho_{0\kappa}$  where  $\rho_{0\kappa}$  is the density of the pure component  $\kappa$  and  $\rho_{C\kappa}^{(i)}$  is the density of component  $C\kappa$  in region  $i$ . In region 3,  $\varphi_C^{(3)} = \rho_C^{(3)} / \rho_{0C}$ , with  $\rho_{0C}$  defined by

$$Z_C / \rho_{0C} = Z_{CA} / \rho_{0A} + Z_{CB} / \rho_{0B} \quad (2-2)$$

with  $Z_{C\kappa}$  the degree of polymerization of block  $C\kappa$ , and  $Z_C = Z_{CA} + Z_{CB}$ . For the homopolymer,  $\varphi_{HA}^{(i)} = \rho_{HA}^{(i)} / \rho_{0A}$ .

Because one of our primary objectives is testing the model against experiment, we use the appropriate reference densities. For polybutadiene, we take<sup>4</sup>

$$\rho_{0A} = 1 / \{54.09[1.0968 + 8.24 \times 10^{-4}(T - 273)]\} \text{ mol cm}^{-3} \quad (2-3)$$

where  $T$  is the temperature in kelvins, and for polystyrene<sup>5</sup>

$$\begin{aligned}\rho_{0B} &= 1 / \{104.15[0.9199 + 5.098 \times 10^{-4}(T - 273) + \\ &\quad 2.354 \times 10^{-7}(T - 273)^2 + \\ &\quad (32.46 + 0.1017(T - 273)) / M_{CB}]\} \text{ mol cm}^{-3} \quad (2-4)\end{aligned}$$

where  $M_{CB}$  is the molecular weight of the B block. Thus, the temperature dependence and, in the case of the polystyrene, the molecular weight dependence of the reference densities are included. The Kuhn statistical lengths for the two components are  $b_A = 0.68$  nm and  $b_B = 0.71$  nm for polybutadiene and polystyrene, respectively.<sup>4</sup>

The fraction of the total volume occupied by region  $i$  is denoted  $G_i^v$ . In terms of the copolymer fractions  $F_M^C$  and  $F_3^C$ , and the overall homopolymer and copolymer volume fractions  $\varphi_{HA}^0$  and  $\varphi_C^0$ , we have

$$\begin{aligned}G_1^v &= (l_B / R)^3 \\ G_2^v &= ((l_A + l_B) / R)^3 - G_1^v \\ G_3^v &= 1 - (G_1^v + G_2^v)\end{aligned}\quad (2-5)$$

and eq 2-1 become

$$\begin{aligned}F_M^C f_B (\varphi_C^0 / G_1^v) + F_1^{HA} (\varphi_{HA}^0 / G_1^v) &= 1 \\ F_M^C f_A (\varphi_C^0 / G_2^v) + F_2^{HA} (\varphi_{HA}^0 / G_2^v) &= 1 \\ F_3^C (\varphi_C^0 / G_3^v) + F_3^{HA} (\varphi_{HA}^0 / G_3^v) &= 1\end{aligned}\quad (2-6)$$

where for each component  $f_\kappa = (Z_{C\kappa} \rho_{0C}) / (Z_C \rho_{0\kappa})$ , and the overall volume fraction of component  $C\kappa$  is  $\varphi_{C\kappa}^0 = f_\kappa \varphi_C^0$ .

We express the free energy per unit volume of the micelles relative to the random state

$$\Delta g = (G_{micelle} - G_{random}) / \rho_{0B} k_B T V \quad (2-7)$$

as a sum of six terms. In (eq 2-7),  $V$  is the volume of the system,  $\rho_{0B}$  a reference density (corresponding to polystyrene in our problem), and  $k_B$  Boltzmann's constant. The first five contributions to  $\Delta g$  are discussed in more detail in ref 2.

The first and largest term accounts for the polymer-polymer interactions. In the random state, the CB copolymer blocks (overall volume fraction  $f_B \varphi_C^0$ ) interact with the CA copolymer blocks ( $f_A \varphi_C^0$ ) and the HA homopolymer. When micelles form, within the core a fraction  $F_M^C$  of the CB blocks interacts with a fraction  $F_1^{HA}$  of homopolymer. Outside the micelles the remaining fraction  $F_3^C$  of CB blocks interacts with the same fraction of CA blocks and the fraction  $F_3^{HA}$  of the homopolymer. The difference in the interaction free energy can be written as follows:

$$\begin{aligned}g_{int} &= -\chi f_B \varphi_C^0 f_A \varphi_C^0 [1 - (F_3^C)^2 / G_3^v] + \\ &\quad \varphi_{HA}^0 (1 - F_M^C F_1^{HA} / G_1^v - F_3^C F_3^{HA} / G_3^v)\end{aligned}\quad (2-8)$$

The Flory  $\chi$  parameter for polystyrene-polybutadiene is based on the work of Roe and Zin<sup>6</sup>

$$\chi_{AB} \equiv \chi = -0.0835 + 73/T \quad (2-9)$$

with  $T$  measured in kelvins.

The interaction between the copolymer CB and CA blocks within the micelle is incorporated via the interfacial term. The expression used is a simple one tested against numerical self-consistent calculations in ref 7, with the modification that in the present case there is no third material as solvent. Anticipating our results, we find that in virtually all cases,  $\varphi_{CB}^{(1)} \geq 0.98$ , so for the interfacial tension we assume  $\varphi_{CB}^{(1)} = 1$ , leading to a free energy contribution

$$g_I = \frac{\gamma}{\rho_0 k_B T} \frac{3l_B^2}{R^3} \quad (2-10)$$

with

$$\gamma/\rho_0 k_B T = (\chi/6)^{1/2} b \quad (2-11)$$

where  $b$  is an average Kuhn statistical length. In these two expressions it is assumed that the molar densities of each pure component  $\rho_{0k}$  are the same,  $\rho_0$ . In the present case we have taken  $\rho_0 = \rho_{0B}$ . The analysis also gives a simple expression for the width of the interface,  $d$

$$d = (2/3\chi)^{1/2} b \quad (2-12)$$

The localization of the molecules involves restricting fractions  $F_i^{HA}$  of homopolymer to regions  $i$ , the fraction  $F_3^C$  of copolymer to region 3, and the fraction  $F_M^C$  of copolymer such that the joints are in the interfacial region between the core and the corona. The entropy of mixing and localization of joints give the following contributions to the free energy:

$$g_s = \frac{\rho_{0A}}{\rho_{0B}} \frac{\varphi_{HA}^0}{Z_{HA}} \{ F_1^{HA} \ln (F_1^{HA}/G_1^v) + F_2^{HA} \ln (F_2^{HA}/G_2^v) + F_3^{HA} \ln (F_3^{HA}/G_3^v) \} \quad (2-13)$$

$$g_J = \frac{\rho_{0C}}{\rho_{0B}} \frac{\varphi_C^0}{Z_C} \left\{ F_M^C \ln \left( \frac{F_M^C R^3}{3l_B^2 d} \right) + F_3^C \ln \left( \frac{F_3^C}{G_3^v} \right) \right\} \quad (2-14)$$

The blocks of the copolymers in the micelles are also stretched along the radial direction, resulting in a decrease in the entropy, the so-called "elastic energy", which is given by the Flory expression

$$g_{el} = \frac{\rho_{0C}}{\rho_{0B}} \frac{\varphi_C^0}{Z_C} \frac{F_M^C}{2} \left\{ \alpha_B^2 + \frac{2}{\alpha_B} + \alpha_A^2 + \frac{2}{\alpha_A} - 6 \right\} \quad (2-15)$$

where

$$\alpha_B = (3/Z_{CB})^{1/2} l_B/b_B$$

$$\alpha_A = (3/Z_{CA})^{1/2} l_A/b_A \quad (2-16)$$

Finally, we include a term which corresponds to the translational entropy of the micelles themselves<sup>3</sup> and is obtained by using a simple lattice model

$$g_{tr} = \frac{\rho_{0C}}{\rho_{0B}} \frac{\varphi_C^0}{N_M Z_C} F_M^C \{ \ln (G_1^v + G_2^v) + (G_3^v/(G_1^v + G_2^v)) \ln G_3^v \} \quad (2-17)$$

where  $N_M$  is the number of copolymer molecules per micelle. This contribution to  $\Delta g$  is generally 2-3 orders of magnitude smaller than each of the others.

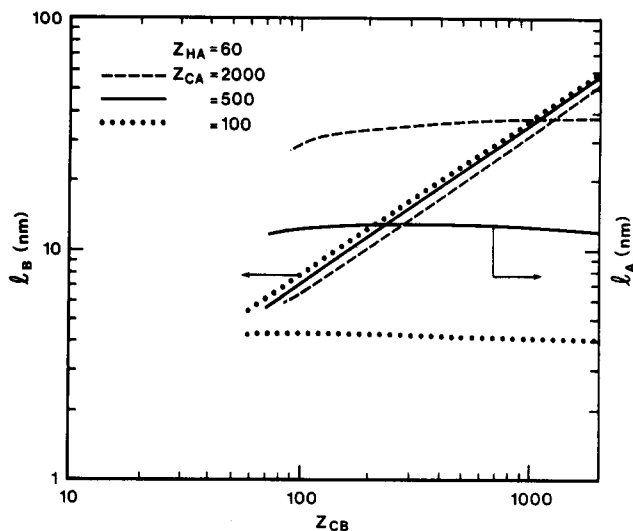


**Figure 2.** Core radius  $l_B$  and corona thickness  $l_A$  as a function of the degree of polymerization (dp) of the core block  $Z_{CB}$ , for homopolymer with (dp)  $Z_{HA} = 60$ , and different dp of the corona block  $Z_{CA}$ . Each curve terminates at the value of  $Z_{CB}$  for which the critical micelle concentration rises to  $\varphi_C^0 = 0.05$ .

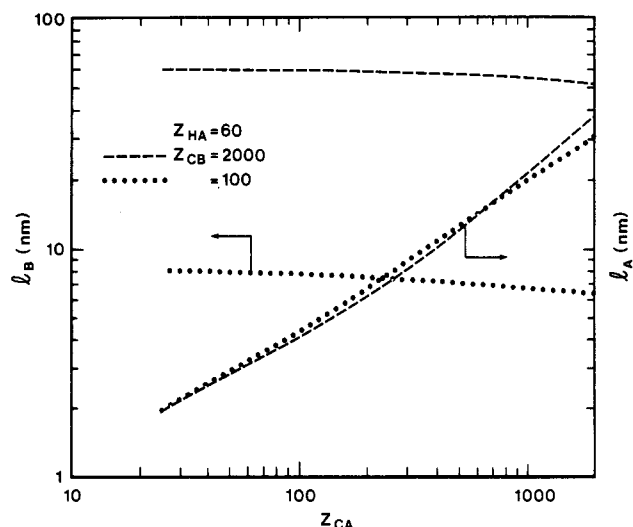


**Figure 3.**  $l_B$  and  $l_A$  as a function of  $Z_{CA}$ , for  $Z_{HA} = 60$  and two values of  $Z_{CB}$ , with  $Z_{CA}$  ranging from 25 to 2000.

The total free energy to be minimized is the sum of the above contributions

$$\Delta g = g_{int} + g_I + g_S + g_J + g_{el} + g_{tr} \quad (2-18)$$

With the condition of incompressibility, eq 1, there are four independent variables, which we found convenient to take as  $l_B$ ,  $l_A$ ,  $R$ , and  $F_M^C$ . The procedure for minimizing the free energy is described in the Appendix of ref 2.

### 3. General Trends and Comparison with Experiment

**a. General Trends.** In this section, we explore the general trends predicted by the model, examining first the dependence of the micelle properties on the various molecular weights and temperature. The micelle cores consist almost entirely of polystyrene blocks of the copolymer; the homopolymer volume fraction satisfies  $\varphi_{HA}^{(1)} < 0.001$  for  $Z_{HA} \geq 60$ , rising to at most 0.02 for  $Z_{HA} = 30$ . Furthermore, away from the critical concentration, most of the copolymers are localized in the micelle; the volume fraction of copolymer remaining in solution is correspondingly small.

Figures 2 and 3 exhibit the dependence of both the core radius  $l_B$  and corona thickness  $l_A$  on the molecular weights

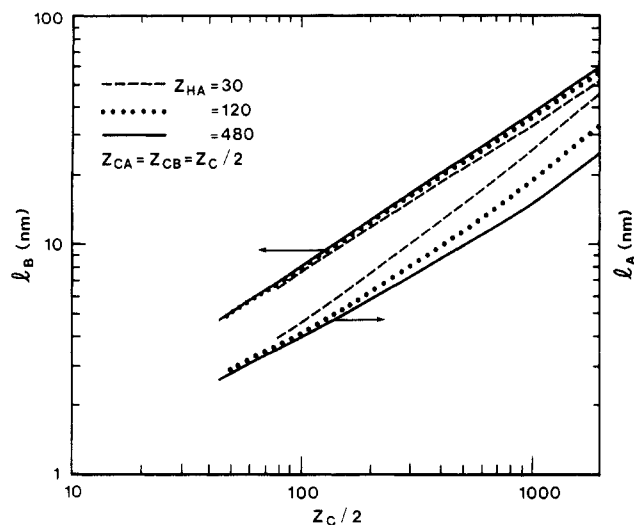


**Figure 4.**  $l_B$  (upper three curves) and  $l_A$  (lower three curves) as a function of the degree of polymerization of each block for  $Z_{CA} = Z_{CB} = Z_C/2$ . As in Figure 1, the curves are terminated on the left at the value for which the critical concentration rises to  $\phi_C^0 = 0.05$ .

of the CB and CA blocks, respectively. For  $l_B$ , a scaling relation is obeyed very closely over the entire range shown, which spans 3 orders of magnitude in molecular weight.

$$l_B \propto Z_{CA}^{\mu} Z_{CB}^{\nu} \quad (3-1)$$

The index  $\nu$  is only slightly dependent on the molecular weights, lying in the range 0.67–0.76. The value of  $l_B$  slowly decreases with increasing  $Z_{CA}$ ,  $-0.1 < \mu < 0$ , although the index  $\nu$  is nearly independent of  $Z_{CA}$ . This does not reflect a change in volume fraction in the core; for the case of  $Z_{HA} = 60$ ,  $\phi_{CA}^{(1)} \geq 0.999$ . Rather, the number of copolymer chains aggregated into each micelle decreases as  $Z_{CA}$  increases.

The corona thickness  $l_A$  also exhibits a power law dependence on  $Z_{CA}$

$$l_A \propto Z_{CA}^{\omega} \quad (3-2)$$

but is a fairly flat (non-power-law) function of  $Z_{CB}$ . However, the index  $\omega$  depends on all of  $Z_{CA}$ ,  $Z_{CB}$ , and  $Z_{HA}$ . The last of these dependencies is clear from Figure 4. For small  $Z_{CA}$ ,  $\omega \simeq 0.5$ , and in fact  $l_A$  is just the unstretched length  $l_A = (Z_{CA}/3)^{1/2} b_A$ . As  $Z_{CA}$  increases, the stretching increases,  $\alpha_A > 1$ , so  $l_A$  increases at a rate faster than  $Z_{CA}^{1/2}$ , and  $\omega$  increases to as much as 0.86 for the cases shown.

Figures 2–4 serve to illustrate that the micelle parameters are determined not only by the total molecular weight, but more importantly by the individual blocks CA and CB. This point is further emphasized by Figure 5, where both  $l_B$  and the total micelle radius ( $l_B + l_A$ ) are plotted as a function of polystyrene fraction for fixed total degree of polymerization  $Z_C$ . The main point is that  $l_B$  and  $l_B + l_A$  can vary greatly for given  $Z_C$ , depending on the relative sizes of the two blocks. In fact, in the case of rather large  $Z_C$ , the total micelle radius for  $Z_C = 2000$  with  $Z_{CB} \gg Z_{CA}$  can be larger than for  $Z_C = 4000$  with  $Z_{CA} \gg Z_{CB}$ . We believe this is not an artifact of the model, because the comparison of our calculations with the experimental results indicates that the theory underestimates the dependences of  $l_B$  on both  $Z_{CB}$  and  $Z_{CA}$ .

On the other hand, if the blocks are varied proportionately, then  $l_B \propto Z_C^{\mu+\nu}$ , and  $l_A \propto Z_C^{\omega}$ , ignoring the small  $Z_{CB}$  dependence of  $l_A$ . This behavior is exhibited in Figure 4. It is interesting to note that for this special case,  $l_B$  exhibits a dependence on  $Z_C$  which is close to the  $2/3$  power law

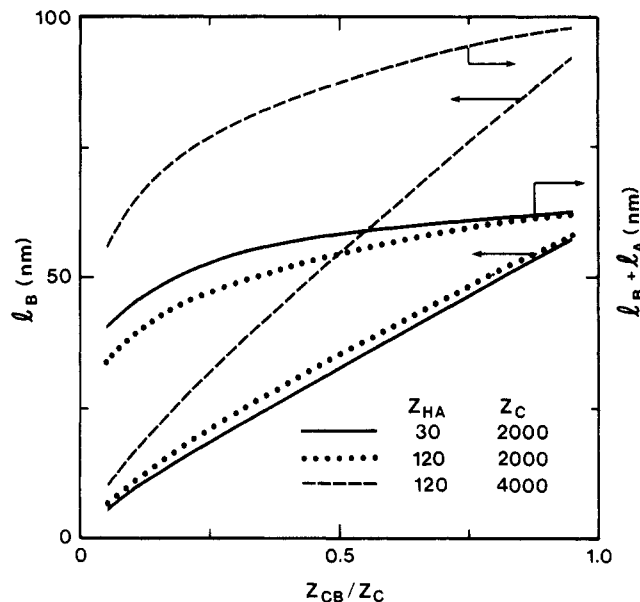


**Figure 5.** Core radius  $l_B$  (lower curve of each pair), and total micelle radius  $l_B + l_A$  (upper curve of each pair) as a function of polystyrene fraction for a given total degree of polymerization  $Z_C$ , for  $0.05 \leq Z_{CB}/Z_C \leq 0.95$ . Near the upper limit of  $Z_{CB}$  approaching  $Z_C$ , micelles may be unstable relative to other morphologies. No attempt has been made to calculate where this might occur.

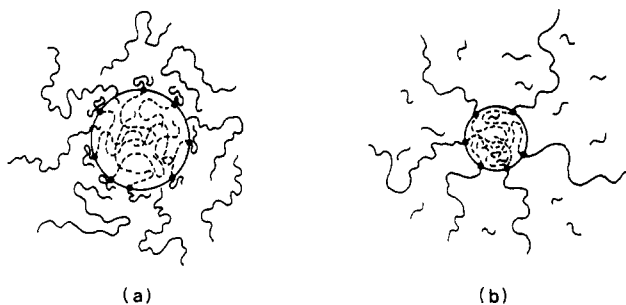


**Figure 6.** Micelle structure for varying  $Z_{HA}$  and  $Z_{CA}$ , with constant  $Z_{CB}$ . If the molecular weight of the homopolymer is large compared with that of the A block of the copolymer, i.e.,  $Z_{HA} \gg Z_{CA}$ , then there is very little stretching of the copolymer in the corona as shown in part a. With  $Z_{HA}$  small relative to  $Z_{CA}$  as shown in part b the stretching of the A block increases as the homopolymer penetrates more into the corona. There is also an accompanying small decrease in the number of molecules per micelle, leading to a reduction in the size of the core, and an increase in the total number of micelles. For very small  $Z_{HA}$ , there may be some penetration of the core by the homopolymer, i.e.,  $\phi_{HA}^{(1)} \simeq 0.02$  when  $Z_{HA} = 30$ .

found in ref 2 as well as in ref 3 for “very strong incompatibilities”. Figure 4 also serves to exhibit the effect of homopolymer molecular weight. Decreasing  $Z_{HA}$  produces a small reduction in  $l_B$ , and a somewhat larger increase in  $l_A$ , particularly for large  $Z_{CA}$ . Consequently the stretching of the corona,  $\alpha_A$ , increases as  $Z_{CA}$  increases or  $Z_{HA}$  decreases.

Figure 6 compares schematically the case of a relatively small  $Z_{CA}$  and large  $Z_{HA}$  (Figure 6a) with the case of large  $Z_{CA}$  and small  $Z_{HA}$  (Figure 6b). In Figure 6a, the short CA blocks are unstretched ( $\alpha_A \simeq 1$ ), with virtually no penetration of the core by the homopolymer. However, when  $Z_{HA}$  is small relative to  $Z_{CA}$ , the large CA blocks become stretched ( $\alpha_A > 1$ ), and there can be some small homopolymer volume fraction  $\phi_{HA}^{(1)}$  in the core. Furthermore, the core radius decreases (see later discussion), and since the core volume fraction  $\phi_{CB}^{(1)}$  remains very nearly unity the aggregation number  $N_M \propto l_B^3/Z_{CB}$  also decreases.

The previous results can be understood physically through a simple analysis. For simplicity consider the case  $b_A = b_B = b$  and  $\rho_{0A} = \rho_{0B}$ , in which case  $f_k = Z_{Ck}/Z_C$  for each block. Since the homopolymer is virtually excluded from the cores, we may put  $\varphi_{CB}^{(1)} = 1$ ,  $F_1^{HA} = 0$ , with little error. Now since  $\varphi_{CB}^{(1)} = f_B \varphi_C^0 F_M^C / G_1^v$ , we have

$$(l_B/R)^3 \simeq (Z_{CB}/Z_C) \varphi_C^0 F_M^C \quad (3-3)$$

thus fixing the ratio  $l_B/R$ . The "interaction" part of the free energy, which is the largest in magnitude, and the only significant negative term contributing to  $\Delta g$ , is given by

$$g_{\text{int}} = -\chi \frac{Z_{CB}}{Z_C} F_M^C \varphi_C^0 \left\{ 1 - \frac{Z_{CB}}{Z_C} \left( 1 - \frac{(F_3^C)^2}{G_3^v} \right) \frac{\varphi_C^0}{F_M^C} \right\} \\ \simeq -\chi (Z_{CB}/Z_C) F_M^C \varphi_C^0 \quad (3-4)$$

which is independent of the micelle parameters  $l_B$  and  $l_A$ .

Equation 3-4 is just the reduction in energy when the fraction  $F_M^C$  of copolymers in the micelle cores no longer interacts with other copolymers or homopolymers.

We also drop the localization term of order  $F_3^C \ln F_3^C$ , as well as the translational entropy of the micelles, and again use  $\varphi_{CB}^{(1)} \simeq 1$ , to give for the total free energy

$$\Delta g \simeq \frac{\varphi_C^0 F_M^C}{Z_C} \left\{ -\chi Z_{CB} + 3Z_{CB} \left( \frac{\chi}{6} \right)^{1/2} \frac{b}{l_B} + \ln \left( \frac{Z_C}{3Z_{CB} \varphi_C^0} \frac{l_B}{d} \right) + \frac{1}{2} \left( \alpha_B^2 + \frac{2}{\alpha_B} + \alpha_A^2 + \frac{2}{\alpha_A} - 6 \right) \right\} \\ + \frac{\varphi_{HA}^0}{Z_{HA}} \left\{ F_2^{HA} \ln \left( 1 - \frac{Z_{CA} F_M^C \varphi_C^0}{Z_C G_2^v} \right) - \ln \varphi_{HA}^0 \right\} \quad (3-5)$$

The entropy of localization of the homopolymer should be negligible if  $Z_{HA}$  is large, or if the volume from which it is being excluded is small, i.e.,  $Z_{CA}$  is small. In this case the entropic contribution from the homopolymer can be dropped from eq 3-3, and the resulting expression minimized with respect to  $l_B$  and  $l_A$ , giving

$$l_B = (\chi/6)^{1/6} Z_{CB}^{2/3} b (1 + O(1/Z_{CB}^{1/3})) \quad (3-6)$$

and for  $Z_{CA} \ll Z_{HA}$

$$l_A = (Z_{CA}/3)^{1/2} b \quad (3-7)$$

The small contribution of  $O(1/Z_{CB}^{1/3})$  above arises from the copolymer localization term in  $\Delta g$ . The physical result is that the *core radius* is determined primarily by a balance between the stretching of the *core block* and the interfacial tension between the core and the corona. On the other hand, when the localization entropy of the homopolymers can be ignored, the CA block is not stretched, and so the *corona thickness* is determined by the unperturbed *corona block*.

If  $Z_{HA}$  is small, or  $Z_{CA}$  large so that the volume of the corona is significant, the configurational entropy of the homopolymer will tend to drive the homopolymer density toward a uniform value by stretching the CA blocks in the corona, thus maximizing the fraction of volume  $G_2^v$ . This can be done by increasing  $l_A$  or decreasing  $R$ , which also results in a smaller core radius  $l_B$ , since  $l_B \propto R$  to a good approximation. Note also that for a given  $\varphi_C^0$ , larger  $Z_{CA}$  (with  $Z_{CB}$  fixed) corresponds to fewer copolymer molecules per unit volume and the overall stretching elastic free energy density is reduced. We thus have the physical picture (see Figure 6) that, for large  $Z_{HA}$  and small  $Z_{CA}$ , the corona consists of unstretched CA copolymer blocks (with homopolymer also present) but that, as  $Z_{HA}$  is de-

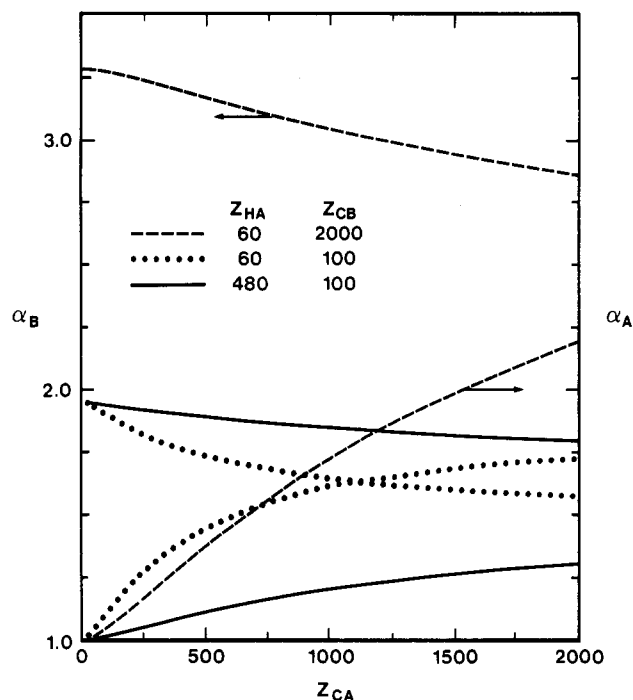


Figure 7. Stretching parameters of the core block,  $\alpha_B$  (upper curve of each pair), and corona block,  $\alpha_A$  (lower curves), as a function of  $Z_{CA}$  for different  $Z_{HA}$  and  $Z_{CB}$ . Although the curves are shown for  $Z_{CA}$  as small as 25, no comparison with other morphologies has been made (as in Figure 5).

creased or  $Z_{CA}$  increased, the localization entropy term drives more homopolymer into the corona, causing it to stretch more, while the core shrinks a small amount. For given  $Z_{HA}$ , the stretching should increase as  $Z_{CA}$  increases because the larger corona means a larger gain in  $G_2^v$  for a given change in  $\alpha_A$ , while for given  $Z_{CA}$ , the stretching increases with decreasing  $Z_{HA}$  due to the larger change in homopolymer entropy.

In the remainder of this section we discuss the stretching parameters  $\alpha_B$  and  $\alpha_A$  defined by eq 2-16. Using the scaling relations for  $l_B$  (eq 3-1), with  $\mu$  ranging from 0 (for small  $Z_{CA}$ ) to  $-0.1$  (see Figure 3), and  $\nu = 2/3$  (eq 3-6) we obtain

$$\alpha_B \propto Z_{CB}^{1/6} \quad Z_{CA} \ll Z_{HA} \\ \alpha_B \propto Z_{CB}^{1/6} / Z_{CA}^{0.1} \quad Z_{HA} \ll Z_{CA} \quad (3-8)$$

Similarly, using  $l_A \propto Z_{CA}^\omega$ , with  $\omega$  ranging from 0.5 (small  $Z_{CA}$ ) to about 0.85 (Figure 3) gives the approximate results

$$\alpha_A \propto Z_{CA}^0 \quad Z_{CA} \ll Z_{HA} \\ \alpha_A \propto Z_{CA}^{0.35} \quad Z_{HA} \ll Z_{CA} \quad (3-9)$$

The exact values of the exponents depend on  $\mu$  and  $\nu$ , but the general behavior is as shown in the full calculation, Figure 7, where it should be noted that each of  $\alpha_A$ ,  $\alpha_B$  range over a factor of about 2.

Finally, the volume fractions in the corona exhibit interesting behavior

$$\varphi_{CA}^{(2)} \propto N_M Z_{CA} / V_2 \quad (3-10)$$

where  $N_M$  is the number of copolymers per micelle and  $V_2$  is the volume of the corona. Using  $l_B \propto Z_{CB}^{2/3}$ ,  $N_M$  is a linear fraction of  $Z_{CB}$ , giving

$$\varphi_{CA}^{(2)} \propto Z_{CA} Z_{CB} / V_2 \quad (3-11)$$

For  $Z_{CA} \ll Z_{CB}$ ,  $l_A \ll l_B$ , then  $V_2 \simeq 4\pi l_B^2 l_A$  which scales as  $Z_{CB}^{4/3} Z_{CA}^{1/2}$  (neglecting the  $Z_{CA}$  dependence of  $l_B$ ). On

**Table I**  
Molecular Characteristics of the Polybutadiene Homopolymers and Polystyrene-Polybutadiene Copolymers (Ref 1)

homopolymer	mol wt	$Z_{HA}$
M1	1600	30
M2	3300	60
M3	6500	120

block copolymer	polystyrene block		polybutadiene block	
	mol wt	$Z_{CB}$	mol wt	$Z_{CA}$
A	14 000	134	29 000	536
B	14 000	134	15 000	277
S	23 000	221	114 000	2108
D	23 000	221	46 000	850

the other hand, for  $Z_{CA} \gg Z_{CB}$ ,  $V_2 \simeq (4/3)\pi l_A^3$ , which scales as  $\sim Z_{CA}^{2.5}$ . Thus

$$\varphi_{CA}^{(2)} \propto Z_{CA}^{1/2}/Z_{CB}^{1/3}, \quad Z_{CA} \ll Z_{CB}$$

$$\varphi_{CA}^{(2)} \propto Z_{CB}/Z_{CA}^{1.5}, \quad Z_{CA} \gg Z_{CB} \quad (3-12)$$

These powers are of course only approximate, but eq 3-12 explains the behavior obtained from the numerical calculation, shown in Figure 8. As  $Z_{CA} \rightarrow 0$ ,  $\varphi_{CA}^{(2)} \rightarrow 0$ , and  $\varphi_{CA}^{(2)}$  is smaller for large  $Z_{CB}$  than for small  $Z_{CB}$ .  $\varphi_{CA}^{(2)}$  reaches a maximum and then decays as a power law depending on the stretching, but now for a given  $Z_{CA}$ ,  $\varphi_{CA}^{(2)}$  is larger for larger  $Z_{CB}$ . There is also a significant dependence on the molecular weight of the homopolymer. For large  $Z_{HA}$ , the corona is stretched less, so the A block is in a thinner corona, causing an increase in  $\varphi_{CA}^{(2)}$ .

It is interesting to compare these results with the conclusions of Leibler et al.<sup>3</sup> They found that for the case of  $Z_{CA} = Z_{CB}$ ,  $\varphi_{CA}^{(2)}$  lies in the range 0.18–0.2 for their choices of  $\chi Z_C$  and  $Z_{HA} = 5Z_C$ . From Figure 8, we see that for each of  $Z_{CA} = Z_{CB} = 100$  and  $Z_{CA} = Z_{CB} = 2000$ ,  $\varphi_{CA}^{(2)}$  is close to this value, but that there exists wide variation for  $Z_{CA} \neq Z_{CB}$ . In fact, these two special cases lie on opposite sides

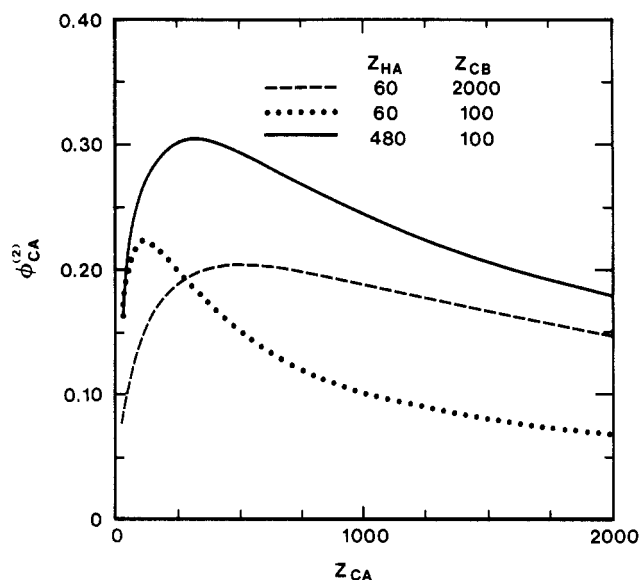


**Figure 8.** Volume fraction of the block copolymers in the corona,  $\varphi_{CA}^{(2)}$ , as a function of  $Z_{CA}$  for different  $Z_{HA}$  and  $Z_{CB}$ .

of maxima in the  $\varphi_{CA}^{(2)}$  vs.  $Z_{CA}$  relationship.

**b. Comparison with Experiment.** Micelle core radii in the polystyrene/polybutadiene system have been measured by using small-angle neutron scattering (SANS) by Selb et al.,<sup>1</sup> who concluded on the basis of the structure of the scattering curves that the micelles were spherical and monodisperse. The molecular characteristics of the three different homopolymers and four different copolymers used in their work are summarized in Table I. Tables II–IV compare the results of Selb et al. with our calculations, using the format and notation introduced by them.

The first feature to note is the degree of overall agreement in the magnitudes of the core radii. The largest discrepancy between experiment and theory is  $\sim 21\%$  and is typically more like  $\sim 10\%$ . Second, the qualitative

**Table II**  
Influence of the Polybutadiene Homopolymer on the Core Radius  $l_B$  (nm) of the Micelle<sup>a</sup>

matrix	$Z_{HA}$	$Z_{CB} = 221, Z_{CA} = 850$						$Z_{CA} = 277, Z_{CB} = 134$		
		cop. D at 2%			cop. D at 5%			cop. B at 2%		
		sample	$l_B^e$	$l_B^t$	sample	$l_B^e$	$l_B^t$	sample	$l_B^e$	$l_B^t$
M1	30	1D2	11.7	11.2	1D5	10.1	11.2	1B2	9.6	8.8
M3	60	3D2	14.3	11.8	3D5	11.5	11.8	3B2	11.5	9.1
M6	120	6D2	15.2	12.4	6D5	13.5	12.4	6B2	12.3	9.3

<sup>a</sup> The superscripts e and t refer to experimental and theoretical values, respectively.

**Table III**  
Influence of the Polybutadiene Content of the Block Copolymer on the Experimental and Theoretical Core Radii,  $l_B^e$  and  $l_B^t$  (nm), of the Micelle

copolymer			2% in matrix M3 ( $Z_{HA} = 60$ )			2% in matrix M1 ( $Z_{HA} = 30$ )		
	$Z_{CB}$	$Z_{CA}$	sample	$l_B^e$	$l_B^t$	sample	$l_B^e$	$l_B^t$
A	134	536	3A2	10.5	8.6	1A2	8.5	8.2
B	134	277	3B2	11.5	9.1	1B2	9.6	8.8
S	221	2108	3S2	12.0	10.9			
D	221	850	3D2	14.3	11.8			

**Table IV**  
Influence of the Total Molecular Weight of the Block Copolymer on the Core Radius  $l_B$  (nm) of the Micelle (Experimental and Theoretical) with  $Z_{CA}/Z_{CB}$  Approximately Constant

copolymer			2% in matrix M1 ( $Z_{HA} \approx 30$ )			2% in matrix M3 ( $Z_{HA} \approx 60$ )		
	$Z_C$	$Z_{CA}/Z_{CB}$	sample	$l_B^e$	$l_B^t$	sample	$l_B^e$	$l_B^t$
D	1070	3.85	1D2	11.7	11.2	3D2	14.3	11.8
A	670	4.00	1A2	8.5	8.2	3A2	10.5	8.6

Table V  
Experimental and Corresponding Theoretical Powers for  
the Core Radii,  $l_B \propto Z_{CA}^\mu Z_{CB}^\nu$ <sup>a</sup>

homo- polymer	copolymer		expt		theory	
$Z_{HA}$	$Z_{CB}$	$Z_{CA}$	$\mu^e$	$\nu^e$	$\mu^t$	$\nu^t$
30	134-221	536-850		0.81		0.70
30	134	277-536	-0.18		-0.09	
60	134-221	536-850		0.75		0.69
60	134	277-536	-0.14		-0.07	
60	221	850-2108	-0.19		-0.09	

<sup>a</sup> The calculation of the experimental values is described in the text. An uncertainty of  $\pm 0.2$  nm in the measured  $l_B$  would produce an uncertainty of  $\sim \pm 0.05$  in  $\mu$  and  $\pm 0.1$  in  $\nu$ .

dependence of  $l_B$  on the degrees of polymerization of the various components is correct:  $l_B$  tends to increase with increasing  $Z_{CB}$  (Tables II-IV), but decreases as either  $Z_{CA}$  (Table III) or  $Z_{HA}$  (Table II) increases. On the other hand, an experimentally observed decrease in  $l_B$  with increasing copolymer concentration is not reproduced by our model, presumably because we do not include interactions between micelles.

The experimental dependence of  $l_B$  on the molecular weights can be quantified through the power law relationship eq 3-1. In Table III, copolymers denoted A and B each have  $Z_{CB} = 136$ , while copolymers S and D each have  $Z_{CB} = 221$ , enabling one to extract the exponent  $\mu$ . As found theoretically and summarized in Table V,  $\mu$  is small and negative and depends a little on (possibly all of)  $Z_{HA}$ ,  $Z_{CB}$ , and the range of  $Z_{CA}$  (see also Figure 3). The experimental values are in the neighborhood of -0.17, about twice the values we predict theoretically for these molecular weights. In Table V we have indicated that an uncertainty in the measurements of  $\pm 0.2$  nm would imply an uncertainty in the extracted index of about  $\pm 0.05$ . This simply indicates how errors in  $l_B$  would be reflected in uncertainties in  $\mu$ .

Having extracted  $\mu$ , we can then obtain  $\nu$  from the data of Table V, in which both  $Z_{CA}$  and  $Z_{CB}$  are varied (with approximately 50% polystyrene by weight in each case). Again there is good agreement between the experimental and theoretical results, with  $\mu$  being 0.75-0.81 experimentally, and somewhat less, 0.68-0.70, theoretically. Note also that the small changes in  $\mu$  and  $\nu$  with  $Z_{HA}$ ,  $Z_{CA}$ , and  $Z_{CB}$  are qualitatively in agreement. As a final check, the scaling relations and extracted indices are found to be consistent with the data of Table II, where  $Z_{CA}$  and  $Z_{CB}$  are varied disproportionately.

#### 4. Critical Micelle Concentration

We specify the critical micelle concentration by the copolymer volume fraction remaining in solution,  $\phi_C^{(3)}$ , when micelles are present. (It is clear from Figure 12 that this is essentially the same as the minimum overall volume fraction  $\phi_C^0$  required for micelles to form.) This quantity is denoted by  $\phi_C^{crit}$ . The main results of the theory are exhibited in Figures 9-12. Figure 9 illustrates the dependence of  $\phi_C^{crit}$  on the molecular weights  $Z_{CB}$ ,  $Z_{CA}$ , and  $Z_{HA}$ . A striking feature is the very strong dependence of  $\phi_C^{crit}$  on the CB block, decreasing by 2 orders of magnitude while  $Z_{CB}$  increases by 50%. By contrast, the  $Z_{CA}$  dependence is much slower, and  $\phi_C^{crit}$  increases with increasing  $Z_{CA}$ . In fact, for small  $Z_{CA}$  there is very little dependence, increasing to approximately  $Z_{CA}^{3/2}$  for very large  $Z_{CA}$  (Figure 9, middle panel). This result again serves to illustrate the importance of distinguishing between the two copolymer blocks, and not restricting attention to only the total molecular weight. From the lower panel of the figure it is also apparent that there is a significant de-

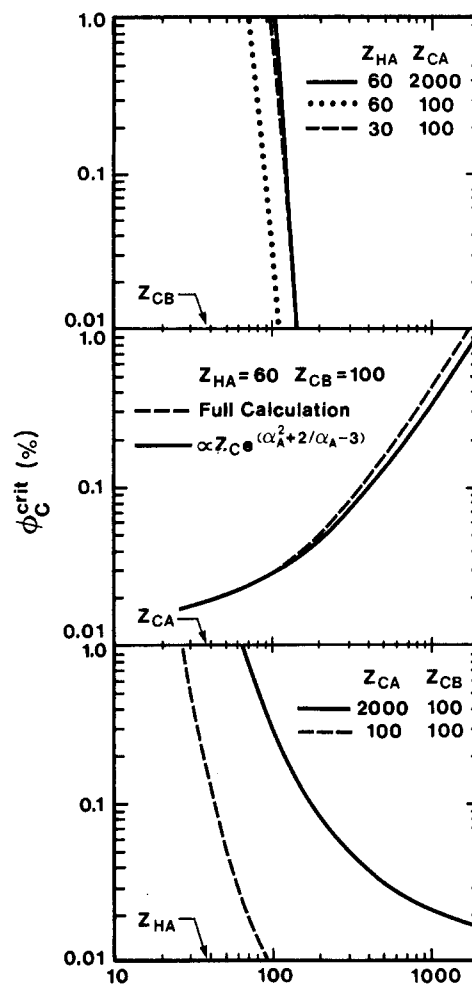


Figure 9. Variation of  $\phi_C^{crit}$  (%) with  $Z_{CB}$  (upper panel),  $Z_{CA}$  (middle panel), and  $Z_{HA}$  (lower panel).

pendence on the homopolymer molecular weight, particularly for small  $Z_{CA}$ .

Much of this general behavior can be obtained analytically. The enthalpic term has little effect on the micelle dimensions, being essentially independent of the size parameters, but it is the predominant term for determining  $\phi_C^{crit}$ . Dropping again the homopolymer localization term and equating the remaining expression for  $\Delta g$  to zero results in an equation for  $\phi_C^{crit}$  with the solution

$$\phi_C^{crit} \approx 0.30 \frac{\chi Z_C}{(\chi Z_{CB})^{2/3}} \exp \left\{ -\chi Z_{CB} + 1.65(\chi Z_{CB})^{1/3} + \frac{1}{2} \left[ 1.65(\chi Z_{CB})^{1/3} + \frac{1.56}{(\chi Z_{CB})^{1/6}} - 3 \right] + \frac{1}{2} \left[ \alpha_A^2 + \frac{2}{\alpha_A} - 3 \right] \right\} \quad (4-1)$$

Each term in the argument of the exponent can easily be identified; in order, they arise from the enthalpy, interfacial tension, stretching of the B block, and stretching of the A block. This equation facilitates understanding the mechanisms determining  $\phi_C^{crit}$ , as well as illuminating the effects of each parameter. It is more general, and for these purposes more useful, than the corresponding one in ref 3.

The occurrence of the exponential and the prefactor are due to the nonlinear copolymer localization term. In order to obtain reasonable magnitudes for  $\phi_C^{crit}$  in this expression, all terms in the exponential must be included (with the exception of the last for small  $Z_{CA}$ ). However, the

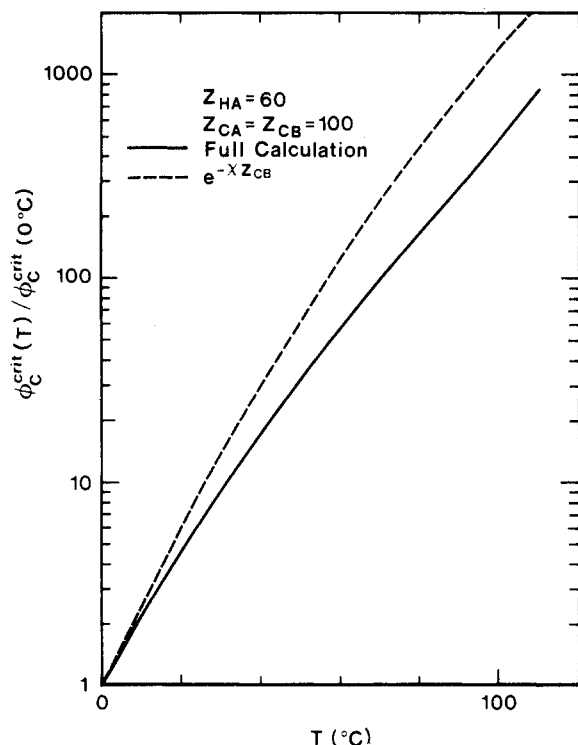


Figure 10. Variation of  $\phi_C^{crit}$  [normalized to  $\phi_C^{crit}(0^\circ\text{C})$ ] with temperature.

dominant  $Z_{CB}$  and temperature dependences arise from only the first term, as seen from Figures 9 (upper panel) and 10. Thus, we have essentially an exponential dependence of the critical concentration on  $\chi Z_{CB}$ .

For small  $Z_{CA}$ ,  $\alpha_A \approx 1$  and the above expression predicts a linear dependence on the total degree of polymerization  $Z_C$ . Note that in this case  $\phi_C^{crit}$  scales with  $Z_{CA}$  in such a way that  $\phi_{CB}^0$  remains constant, since the overall volume fraction of CB block is related to the overall copolymer volume fraction  $\phi_C^0$  by  $\phi_{CB}^0 = (Z_{CB}/Z_C)\phi_C^0$ . On the other hand, for large  $Z_{CA}$ , the increase in CA block stretching ( $\alpha_A$ ) with  $Z_{CA}$  leads to an additional dependence, consistent with the curve shown in the middle panel of Figure 9. Furthermore, a smaller  $Z_{HA}$  induces a larger  $\alpha_A$  for given  $Z_{CA}$ , indicating an increase in  $\phi_C^{crit}$  with smaller  $Z_{HA}$ , again consistent with the figures. Of course, to properly include the homopolymer effects, the relevant entropy terms would need to be retained. In particular the lower panel of Figure 9 is not correctly reproduced by eq 4-1. Here the solid and dotted lines show a strong decrease in  $\phi_C^{crit}$  with increasing homopolymer molecular weight, indicating the importance of the homopolymer entropy. The difference between the two curves reflects the  $Z_{CA}$  dependence illustrated in the middle panel.

Within our model there is a very strong exponential dependence of  $\phi_C^{crit}$  on the temperature  $T$  as illustrated in Figure 10. For  $Z_{HA} = 60$ ,  $Z_{CA} = Z_{CB} = 100$ ,  $\phi_C^{crit}$  increases by 3 orders of magnitude as the temperature is raised from 0 to 100  $^\circ\text{C}$ . The approximation  $\phi_C^{crit} \propto \exp(-\chi Z_{CB})$  works well for changes in  $Z_{CB}$  as well as temperature as shown explicitly in Figure 10. One consequence of this is that, for a given overall volume fraction  $\phi_C^0$ , the volume fraction remaining in solution decreases exponentially as the temperature is decreased.

The last two diagrams further examine the degree to which the copolymers aggregate into micelles. Figure 11 illustrates the continuous increase in  $\phi_C^{(3)}$ , and corresponding decrease in  $F_M^C$ , as the temperature is raised toward the critical temperature. We point out that, even

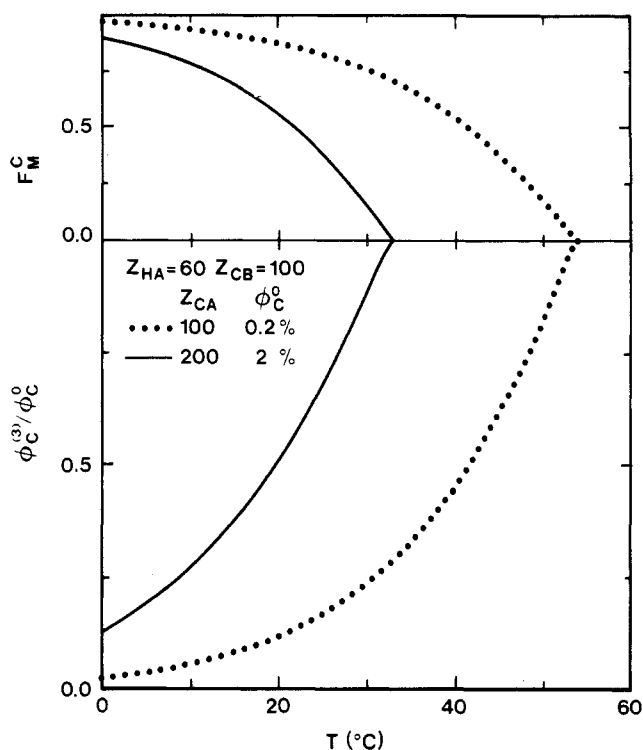


Figure 11. Variation of the volume fraction of copolymers in solution,  $\phi_C^{(3)}$ , and the fraction of copolymers aggregated into micelles,  $F_M^C$ , with temperature. In each case the overall copolymer volume fraction  $\phi_C^0$  is chosen so that the critical temperature for micelle formation is not far above room temperature.

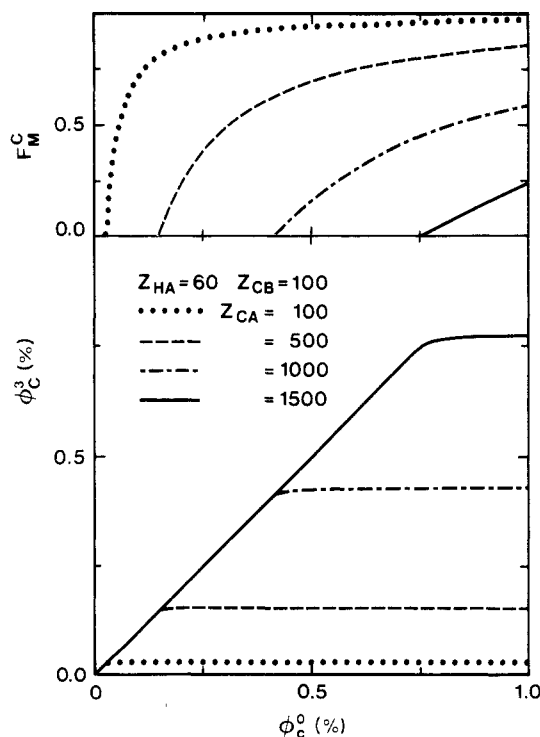


Figure 12. Variation of  $\phi_C^{(3)}$  and  $F_M^C$  with overall copolymer volume fraction  $\phi_C^0$ , at room temperature.

as the transition is approached, the micelle parameters do not change significantly (there is some small smooth change due to the changing  $\chi$ ); nor is there any further penetration of the micelles by the homopolymer. Rather, the number of micelles per unit volume decreases, with the unit cell radius  $R$  diverging at the critical temperature.

Figure 12 exhibits  $\phi_C^{(3)}$  and  $F_M^C$  as a function of  $\phi_C^0$ . For  $\phi_C^0 < \phi_C^{crit}$ , there are no micelles, so  $\phi_C^{(3)} = \phi_C^0$ . Above



$\varphi_C^{\text{crit}}, \varphi_C^{(3)} = \varphi_C^{\text{crit}}$ , and all excess copolymer molecules aggregate into micelles. For the case of large  $Z_{CA}$ , there is a range of  $\varphi_C^0$  just below  $\varphi_C^{\text{crit}}$  for which micelles exist, but addition of more copolymer results in a slight increase in  $\varphi_C^{(3)}$ . However, this corresponds to a small range of  $\varphi_C^0$ , and the transition becomes sharper with decreasing  $Z_{CA}$ .

## 5. Conclusions

The experimental measurements by Selb. et al.<sup>1</sup> of the core radius were analyzed and found to be consistently described by a scaling relationship  $l_B \propto Z_{CA}^\mu Z_{CB}^\nu$ , with  $-0.19 \leq \mu \leq -0.14$  and  $0.75 \leq \nu \leq 0.81$ . This behavior was well reproduced by the model, except that the magnitude of each of the exponents was slightly smaller, with  $-0.10 \leq \mu \leq -0.07$  and  $0.68 \leq \nu \leq 0.70$ . The small variations in both the experimental and theoretical exponents exhibited the same trends with respect to changes in homopolymer and copolymer molecular weights. It was emphasized that the dominant dependence of  $l_B$  is on the core block  $dp$   $Z_{CB}$ , not the total  $Z_C$ , and in fact  $l_B$  tends to *decrease* if the CA block molecular weight increases, rather than increase as it does when the CB block molecular weight increases. More generally,  $l_B$  is not a single-valued function of only the total molecular weight.

This behavior was evident throughout calculations over large ranges of molecular weight, with  $Z_{CB}$  and  $Z_{CA}$  varying up to 2000. Physically, the core radius is primarily determined by a balance between the stretching energy of the core and the interfacial free energy. In the corona, different mechanisms are important. For  $Z_{HA} \gg Z_{CA}$ , there is little stretching of the blocks in the corona, so that  $l_A \approx (Z_{CA}/3)^{1/2} b_A$ . However, for smaller  $Z_{HA}$  or larger  $Z_{CA}$ , the homopolymer penetrates more into the corona, stretching the A blocks with the result that  $l_A$  increases faster than  $Z_{CA}^{1/2}$ . This also has the effect of shrinking

the core radius,  $l_B \sim Z_{CA}^\mu$ , where  $\mu$  is small and negative.

In all cases, there was almost no homopolymer in the core of the micelle, and far from the critical concentration relatively little copolymer remaining in the region between micelles. The critical concentration itself was found to have primarily an exponential dependence on  $\chi_{AB} Z_{CB}$ , and a simple expression for  $\varphi_C^{\text{crit}}$  was exhibited. Physically, the  $Z_{CB}$  dependence arises from the enthalpic interaction of the CB block of the copolymer with the homopolymer. By contrast,  $\varphi_C^{\text{crit}}$  *increases* as  $Z_{CA}$  increases. This reflects primarily the dependence of overall copolymer volume fraction  $\varphi_C^0$  with  $Z_{CA}$  for a given  $\varphi_{CB}^0$ .

Throughout, the composition of the copolymer, not just the total molecular weight, has been found to be important. Analyses which make specific assumptions, such as  $Z_{CA} = Z_{CB}$ , must be considered incomplete.

**Acknowledgment.** M.D.W. thanks the Natural Sciences and Engineering Research Council of Canada for the award of a Senior Industrial Fellowship and the Xerox Research Centre of Canada for hospitality during the course of this work.

**Registry No.** Polybutadiene (homopolymer), 9003-17-2; (butadiene)-(styrene) (copolymer), 9003-55-8.

## References and Notes

- Selb, J.; Marie, P.; Rameau, A.; Duplessix, R.; Gallot, Y. *Polym. Bull.* **1983**, *10*, 444.
- Noolandi, J.; Hong, K. M. *Macromolecules* **1983**, *16*, 1443; **1982**, *15*, 482.
- Leibler, L.; Orland, H.; Wheeler, J. C. *J. Chem. Phys.* **1983**, *79*, 3550.
- Brandrup, J., Immergut, E. G., Eds. "Polymer Handbook"; Interscience: New York, 1966.
- Richardson, M. J.; Savill, N. G. *Polymer* **1977**, *18*, 3.
- Roe, R.-J.; Zin, W.-C. *Macromolecules* **1980**, *13*, 1221.
- Hong, K. M.; Noolandi, J. *Macromolecules* **1981**, *14*, 736.

# Thermodynamics of Phase Separation in Polymer Mixtures

Giorgio Ronca\* and Thomas P. Russell

IBM Research Laboratory, San Jose, California 95193. Received March 13, 1984

**ABSTRACT:** Phase equilibria and spinodal decomposition of polystyrene/polybutadiene blends are investigated by using the Flory-Huggins approximation and the Landau expansion of the free energy. Experimental cloud point curves extrapolated to infinitely slow heating and cooling rates are adequately explained by assuming a suitable power law dependence of the effective interaction parameter  $\bar{\chi}$  on temperature. Theoretical arguments stressing the configurational effects of a concentration gradient yield an expression for the gradient term that is substantially different from the de Gennes-Pincus formula. According to our calculations, the gradient term is a homogeneous quadratic form of the three interaction parameters of the binary mixture and has a much stronger molecular weight dependence. Finally, the interphase thickness and surface tension are evaluated near the critical point. In this limit, provided  $\bar{\chi}$  has a power law dependence on temperature, the surface tension is found to be proportional to  $[(T_c - T)/T_c]^{3/2} M^{-1/2} g(M)$ , where  $g(M)$  is a constant only if all of the interaction parameters have the same temperature dependence.

## Introduction

The spontaneous phase separation of amorphous glass and metal mixtures via a spinodal mechanism has been extensively studied. Since the initial work of Cahn and Hilliard,<sup>1</sup> there have been numerous experimental and theoretical treatments of this problem. As is evidenced by the substantial amount of current research in this field, it is apparent that even for these small-molecule mixtures a complete description of the kinetics of phase separation is still not available.

In contrast polymer/polymer mixtures have received relatively little attention. This is due in part to the small number of systems accessible to experimental observation.

Investigations on the phase separation kinetics in some high<sup>2-4</sup> and low<sup>5-8</sup> molecular weight polymer mixtures have recently appeared in the literature. Joanny,<sup>9</sup> de Gennes,<sup>10</sup> and, later, Pincus<sup>11</sup> attempted to treat spinodal phase separation in polymers theoretically. Using scaling and reptation arguments they obtained a modified Cahn-Hilliard expression for the fluctuation wavelength amplification factor describing both the thermodynamics and kinetics of phase separation. Their treatments predict the dominant features of the process; however, agreement between theory and experiment is not quantitative.

Recent experimental studies on the spinodal decomposition of some low<sup>8</sup> and high<sup>12</sup> molecular weight polymer